Spin-Density and Charge-Density Excitations in the Paramagnetic Phase of Semiconductor Double Quantum Well Systems

P. G. Bolcatto* and C. R. Proetto

Centro Atómico Bariloche and Instituto Balseiro, 8400 S. C. de Bariloche, Río Negro, Argentina

(Received 2 December 1999)

The interplay of tunneling, Coulomb coupling, and many-body effects on the charge-density excitation (CDE) and spin-density excitation (SDE) of double quantum well systems has been analyzed. For increasing interwell distances, the system moves from the strong-tunneling regime (one-well limit) towards the zero tunneling but still strongly Coulomb-coupled regime, passing by the intermediate regime of a small but finite tunneling-induced gap ($\lesssim$1 meV). Important renormalizations due to many-body effects are found in the long-wavelength limit of the CDE and SDE, with the former exhibiting a logarithmic correction to the single-particle linear dependence on the tunneling-induced gap, and the latter exhibiting a soft mode in the weak-tunneling, low-density regime. The oscillator strength of the SDE soft mode has been calculated and found to be clearly measurable.

PACS numbers: 73.20.Mf, 71.45.Gm, 73.20.Dx

One of the driving forces behind the intense experimental and theoretical activity in the area of low-dimensional semiconductor heterostructures are the multiple and sometimes unexpected manifestations of many-body effects in these systems. The two-dimensional electron gases (2DEG) are, in principle, ideally suited for this research, mainly due to the extremely high quality of the samples, the possibility of changing the electronic density in a controlled way, and the increase of interactions due to the reduced dimensionality [1]. A prime example was the discovery of the fractional quantum Hall effect. In this case, many-body effects are enhanced as a consequence of the application of strong (quantizing) magnetic fields perpendicular to the 2DEG, which quenches the kinetic energy. A zero-field alternative, which is the subject of this paper, is the study of double quantum well (DQW) systems. It has been predicted that these systems should exhibit a rich *ground-state* phase diagram, in the parameter space defined by the interwell distance (tunneling) and low electronic densities (lower than $0.5 \times 10^{11}/\mathrm{cm}^2$) [2,3]. Paramagnetic (P), antiferromagnetic (AF), and ferromagnetic ground states were found as the systems moved towards lower densities and for intermediate barrier widths ($\sim$60 Å). As a crucial step aimed to provide a full understanding of the phenomena, we present here the *excitation spectra* (collective modes) of the system in the P phase at zero temperature. Here there are two varieties of *uncoupled* collective modes: charge density excitations (CDE), or plasmons, and spin density excitations (SDE). Both of them are directly and independently measurable physical magnitudes, for instance, via inelastic-light-scattering (ILS) experiments [4].

All of the results presented below have been performed within the framework of the density functional theory, in its local spin-density approximation (LSDA) [5]. In order to obtain the elementary excitations of the system, the calculation proceeds in two steps. First, we characterize the ground state of the DQW system. This consists of a self-consistent calculation on the effective one-dimensional Schrödinger and Poisson equations along the DQW growth direction (z). The output of such calculation is the self-consistent electronic structure of the DQW system, consisting of the subband energies E_i, Fermi energy E_F, wave functions $\phi_i(z)$, and subband electronic densities n_i; here, $i = 1, 2, 3, \ldots$ denotes the subband index, with $i = 1$ corresponding to the ground (symmetric) subband, $i = 2$ corresponding to the first-excited (antisymmetric) subband, etc. We define $\Delta_{\mathrm{SAS}} = E_2 - E_1$ as the tunneling-induced gap between the two lowest subbands. The second step of the calculation starts from this ground-state information. We apply here the so-called time dependent local spin-density approximation (TDLSDA) [5], which is a linear response theory which generalizes the well-known time dependent Hartree approximation (TDHA) or random phase approximation. The TDLSDA includes exchange and correlation in the calculation of the collective modes of the system, as its input is the LSDA ground-state eigenvalues (subband level structure) and eigenvectors (self-consistent wave functions). The linear response theory also contemplates the perturbation of the exchange-correlation potential.

We start by presenting the results for a GaAs/$\mathrm{Al}_x\mathrm{Ga}_{1-x}\mathrm{As}$ DQW system in the zero-tunneling regime $\Delta_{\mathrm{SAS}} = 0$, which is reached for barrier widths greater than approximately 100 Å. This regime displays two different types of plasmons: "optical," with a dispersion relation $\omega_+(q \to 0) \to \alpha\sqrt{q}$, and "acoustic," with a dispersion relation $\omega_-(q \to 0) \to \beta q$. $\mathbf{q}$ is the in-plane wave vector of the CDE's. The optical (acoustic) mode corresponds to a plasmon for which the charge-density oscillations in the two layers are in phase (out of phase). The optical mode is the standard plasmon of a single isolated quantum well [6], while the acoustic mode is a unique feature brought by the interwell Coulomb interaction [7].

We display in Fig. 1 the full dispersion relation for these two modes and compare it with available experimental data

 0031-9007/00/85(8)/1734(4)$15.00

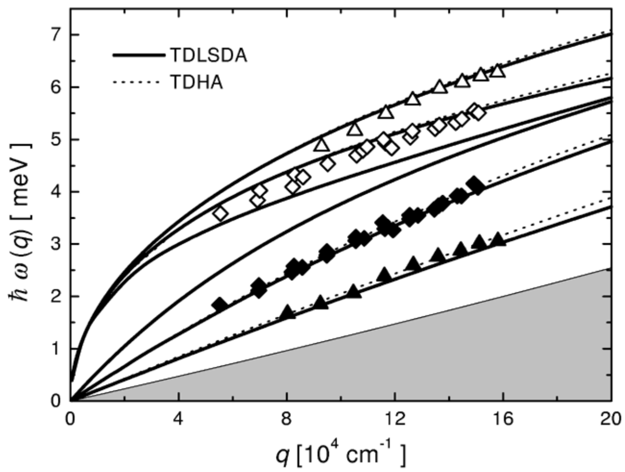

FIG. 1. Dispersion relations for the optical $\omega_+(q)$ (three upper curves) and acoustic $\omega_-(q)$ (three lower curves) plasmons in the zero-tunneling regime. Points are experimental data from Ref. [8]. Triangles: $d_b = 125$ Å and $d_w = 180$ Å. Diamonds: $d_b = 600$ Å and $d_w = 200$ Å. The two curves without experimental data correspond to $d_b = 2000$ Å and $d_w = 140$ Å. The shaded area represents the particle-hole continuum [single-particle excitations (SPE)]. This one-parameter agreement has been achieved with a total density ($N_S = 3.3 \times 10^{11}$ cm^2), about 29% higher than the quoted value, determined from Shubnikov–de Hass measurements *without illumination,* and 16% lower than the results emerging from calculations in Ref. [8].

[8]. Only one adjustable parameter, the total density N_S, has been used to obtain a remarkable agreement between experiment and theory; this is in agreement with earlier calculations which give a simpler treatment to many-body effects [8]. The following points are should be noted: (i) $\omega_+(q)$ and $\omega_-(q)$ have opposite behaviors as the interwell distance d_b increases. In the limit of two Coulomb-decoupled wells, both modes should merge into a single mode with a frequency given by $\omega_+(q \to 0) \to \alpha\sqrt{q}/2$. Nevertheless, even for $d_b = 2000$ Å, the system is still far from the Coulomb-decoupled regime. This zero tunneling but strongly Coulomb-coupled regime has been intensively studied due to its connection with electron-drag transport effects in DQW systems [9]; (ii) many-body effects on both types of plasmons are small in this relatively high-density regime. We have checked that the acoustic plasmon remains stable even in the low-density ($N_S = 0.35 \times 10^{11}/\text{cm}^2$), large-$q$ regime ($q/k_F \simeq 0.6$), differing from earlier results [10] but in agreement with recent calculations [11].

Moving towards the tunneling-dominated regime $\Delta_{\text{SAS}} \neq 0$ [12], we display in Fig. 2 the long-wavelength results for the intersubband elementary excitations of DQW systems with $d_b = 20$ Å and $d_b = 40$ Å. A comparison with Fig. 1 reveals the profound impact that tunneling has on the collective modes of the system. In the first place, the zero-tunneling acoustic plasmon $\omega_-(q)$ evolves from a gapless linear dependence on q to a finite-

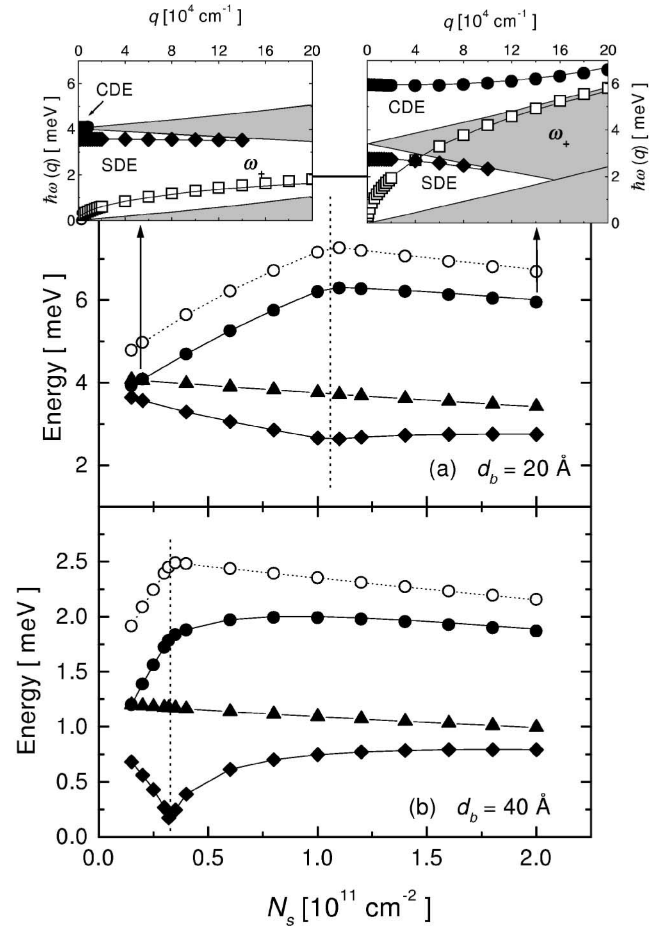

FIG. 2. Total density dependence of Δ_{SAS} (triangles), $\hbar\omega_{\text{CDE}}(0)$ (circles), and $\hbar\omega_{\text{SDE}}(0)$ (diamonds), for two different barrier widths; in both cases, $d_w = 140$ Å. The solid (open) circles are TDLSDA (TDHA) results. The two upper insets are the *full* dispersion relations of CDE, SDE, and ω_+ (squares) collective modes for densities indicated by arrows. The vertical lines separate the one-subband regime (left) from the two-subband regime (right). Here and in Fig. 3 the lines joining points correspond to analytical expressions in the second order long-wavelength limit, but using the *calculated* values for Δ_{SAS}, Δn, γ_{CDE}, and γ_{SDE}.

gap dispersionless mode in the presence of tunneling [13], which, to avoid confusion, we prefer hereafter to denote as $\omega_{\text{CDE}}(q)$. Within the TDLSDA we obtain in the $q \to 0$ limit the following analytical result:

$$\hbar\omega_{\text{CDE}}(q \to 0) \to \Delta_{\text{SAS}}\left(1 + \frac{2\gamma_{\text{CDE}}\Delta n}{\Delta_{\text{SAS}}}\right)^{1/2}, \qquad (1)$$

with γ_{CDE} being a many-body parameter which includes positive (Hartree) and negative (exchange-correlation) contributions, and $\Delta n = n_1 - n_2 \geq 0$. From Eq. (1), the gross features of $\omega_{\text{CDE}}(0)$ are easy to understand. At high densities the Hartree contribution is much larger than the exchange-correlation correction, $\gamma_{\text{CDE}} > 0$, and $\hbar\omega_{\text{CDE}}(0)$ is almost a factor of 2 above its undressed value Δ_{SAS}. However, by decreasing the total density, Hartree and exchange-correlation contributions become comparable, and an interesting situation is presented in which $\hbar\omega_{\text{CDE}}(0)$ approaches its bare value Δ_{SAS} through a many-body driven strong renormalization of the parameter γ_{CDE}. This behavior is clearly seen in the left inset of Fig. 2a [14]. The second important feature is the appearance of a SDE, which does not exist in the zero-tunneling regime. The long-wavelength limit of this mode is also given by Eq. (1), but, since Hartree corrections are absent for this mode, γ_{CDE} is replaced by γ_{SDE} (<0); this explains why this mode appears below Δ_{SAS}. The nonmonotonous behavior of $\omega_{\text{CDE}}(0)$ and $\omega_{\text{SDE}}(0)$ is also a consequence of tunneling: in the two-subband ($2S$) regime the phase-filling factor $n_1 - n_2$ increases by decreasing the total density N_S ($N_S = n_1 + n_2$), which leads to a smooth increase (decrease) of $\omega_{\text{CDE}}(0)$ $[\omega_{\text{SDE}}(0)]$. However, in the one-subband ($1S$) regime the phase-filling factor reduces to $n_1 = N_S$, which leads now to a decreasing (increasing) behavior of $\omega_{\text{CDE}}(0)$ $[\omega_{\text{SDE}}(0)]$ with density. As a consequence, a minimum develops in the long-wavelength limit of the SDE. With this understanding, the way to optimize (enhance) the development of this minimum in $\omega_{\text{SDE}}(0)$, which could lead to its experimental observation is then quite clear: the relative importance of the second term against the first should be increased in Eq. (1). To achieve this, one can tune Δ_{SAS} to smaller values (increasing d_b, for instance). An example of this situation is displayed in Fig. 2b, corresponding to $d_b = 40$ Å, $\Delta_{\text{SAS}} \simeq 1$ meV, which can be qualified as the weak-tunneling regime. The sharp minimum could be interpreted as a SDE soft mode which signals a spontaneous breaking of the spin SU(2) symmetry of the P phase towards some nontrivial spin-ordered phase [2]. The family of collective modes in this tunneling-dominated regime is completed by the intrasubband optical mode $\omega_+(q)$, which, besides being robust against many-body effects, is also insensitive to tunneling, as the coefficient α in $\omega_+(q)$ is independent of Δ_{SAS} and γ_{CDE}.

We display in Fig. 3 the behavior of the collective modes as a function of Δ_{SAS} (or d_b). In the strong-tunneling regime $\Delta_{\text{SAS}} \gg 1$ meV, both CDE and SDE merge towards the undressed value Δ_{SAS}, the convergence being slower for larger densities. This is easily understood from Eq. (1), since for large Δ_{SAS} and in the $1S$ regime both $\hbar\omega_{\text{CDE}}(0)$ and $\hbar\omega_{\text{SDE}}(0)$ have a leading term linear in Δ_{SAS}. However, both modes depart considerably from Δ_{SAS} by decreasing the tunneling, although the particular behaviors in the weak-tunneling regime are very different. Starting with the CDE's, the kink denotes a change of regime from a $1S$ to a $2S$ situation. The critical Δ_{SAS} for the change of regime is $\Delta_{\text{SAS}}^c = \pi\hbar^2 N_S/m^*$. The large increase in $\hbar\omega_{\text{CDE}}(0)/\Delta_{\text{SAS}}$ for $\Delta_{\text{SAS}} \to 0$ is related to the strong dependence of γ_{CDE} with d_b through the long-range Hartree contribution, which in turn translates into a logarithmic singularity of the type $\{\ln|\Delta_{\text{SAS}}(d_b)/\Delta_{\text{SAS}}(0)|\}^{1/2}$

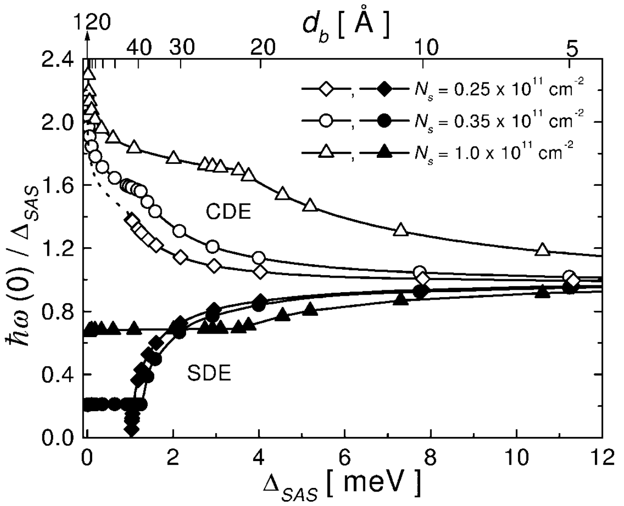

FIG. 3. Tunneling-strength dependence of $\hbar\omega_{\text{CDE}}(0)/\Delta_{\text{SAS}}$ (open symbols) and $\hbar\omega_{\text{SDE}}(0)/\Delta_{\text{SAS}}$ (solid symbols), for three different densities. Kinks at $\Delta_{\text{SAS}} \simeq 0.89$, 1.25, and 3.57 meV correspond to the $1S \to 2S$ transition. CDE obtained from a metastable paramagnetic phase are denoted by a dashed line for the lowest density.

against a $\sqrt{\Delta_{\text{SAS}}}$ dependence predicted previously [13]. In our case, *we take into account tunneling exactly,* which *always* leads to a $2S$ regime for weak enough tunneling. Thus, the $\sqrt{\Delta_{\text{SAS}}}$ weak-tunneling $1S$ regime is replaced by the logarithmic correction discussed above and clearly displayed in Fig. 3. For a full discussion of this point, see Ref. [15]. It is also interesting to note the radically different behavior of the SDE's: for the two higher densities, $\hbar\omega_{\text{SDE}}(0)/\Delta_{\text{SAS}}$ attains a constant value as soon as the second subband becomes occupied [16], while, for the lowest density, the system never reaches the occupied $2S$ regime, and consequently $\hbar\omega_{\text{SDE}}(0)/\Delta_{\text{SAS}}$ goes all the way to zero, signaling the appearance of a magnetic instability [2,3].

These results for the excitation spectra are fully consistent with the ground-state calculations of Ref. [3]. According to the phase diagram of Fig. 1 in that reference, for $N_S = 1$ and $0.35 \times 10^{11}/\text{cm}^2$ the P phase remains stable all the way from the strong- to the weak-tunneling regime. For $N_S = 0.25 \times 10^{11}/\text{cm}^2$, however, and for $d_b \gtrsim 42.3$ Å, the P phase suffers a *second order* instability towards an AF phase. This instability happens in the vicinity of the $1S \to 2S$ transition because the AF ground state corresponds to the localization of, say, electrons with spin up in the left well and electrons with spin down in the right well, which is achieved through an exchange-correlation-induced mixing of the symmetric and antisymmetric subbands of the P phase. If Δ_{SAS} is too large ($\gtrsim$1 meV) this mixing gives a large increase of the kinetic energy along the z direction, and the instability does not occur. From the point of view of the SDE, the instability happens because in the $1S$ regime ω_{SDE} reaches zero at the critical $\Delta_{\text{SAS}}^{\text{ins}} = -2\gamma_{\text{SDE}} N_S$. Both points of view are

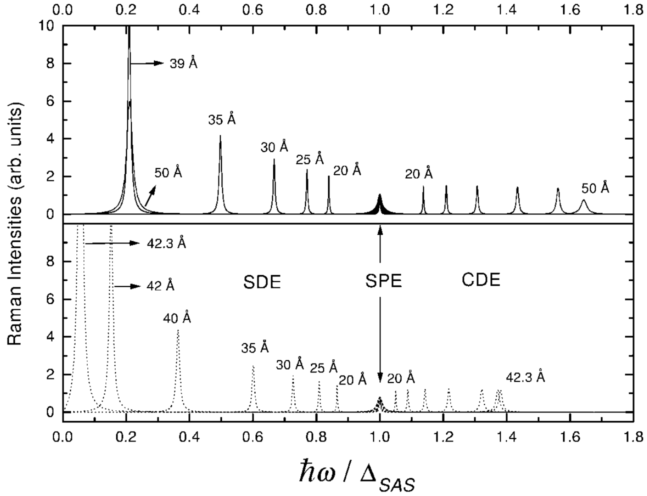

FIG. 4. Charge-density (CDE), spin-density (SDE), and single-particle excitations (SPE) Raman intensities. Solid line: d_b = 20, 25, 30, 35, 39, and 50 Å for $N_s = 0.35 \times 10^{11}$ cm^{-2}. Dashed line: d_b = 20, 25, 30, 35, 40, 42, and 42.3 Å for $N_s = 0.25 \times 10^{11}$ cm^{-2}. The wave vector of the incident radiation is $q_l = 1.6 \times 10^5$ cm^{-1}.

complementary, but the elementary excitation calculations of this paper are *directly* related to the experimental detection of this instability.

In order to assess the feasibility of the observation of this spontaneous breaking of the spin symmetry, we display in Fig. 4 the CDE and SDE Raman intensities for the two lowest densities of Fig. 3. The first point to note is that while far from the instability region both CDE and SDE signals are of comparable magnitude, the SDE signal becomes very large as the system approaches the $1S \rightarrow 2S$ transition. For the higher density, however, the instability is not reached and the SDE Raman intensities display a nonmonotonous behavior, with an intensity maximum around the $1S \rightarrow 2S$ transition. For the lower density, the SDE Raman intensities suffer a monotonous and dramatic increase as the instability is approached by increasing d_b. The results of this figure suggest that, if it is possible to tune the DQW parameters to this low-density and weak-tunneling regime, the associated instability should be clearly measurable by optical experiments with the cross section proportional to these Raman intensities, as, for instance, ILS.

In conclusion, many-body effects on the collective modes in the paramagnetic phase of double quantum well systems have been analyzed, at zero temperature. By applying the time dependent local spin-density approximation we calculate the excitation spectra from the zero-tunneling to the strong-tunneling regime, accounting exactly for tunneling between both wells. At the first limit we found excellent agreement with recent experimental data for plasmon dispersion relations and we conclude that the exchange-correlation corrections are small. Striking effects are predicted in the weak-tunneling regime, such as a logarithmic correction for the intersubband plasmon, and a pronounced softening of the intersubband spin-density channel, signaling towards an instability of the paramagnetic phase of the double quantum well system. The Raman intensities of this soft mode have been calculated, and found to be measurable by inelastic-light-scattering experiments.

This work was partially supported by the CONICET under Grant No. PIP 0473/98 and the ANPCYT under Grant No. PICT97 03-00121-02152. P. G. B. acknowledges the financial support received from FOMEC No. 331, UNL.

*Permanent address: Facultad de Formación Docente en Ciencias and Facultad de Ingeniería Química, Universidad Nacional del Litoral, Sgo. del Estero 2829, 3000 Santa Fe, Argentina.

[1] T. Ando, A. B. Fowler, and F. Stern, Rev. Mod. Phys. **54**, 437 (1982).
[2] S. Das Sarma and P. I. Tamborenea, Phys. Rev. Lett. **73**, 1971 (1994).
[3] F. A. Reboredo and C. R. Proetto, Phys. Rev. Lett. **79**, 463 (1997); F. A. Reboredo and C. R. Proetto, Phys. Rev. B **58**, 7450 (1998).
[4] A. Pinczuk and G. Abstreiter, in *Light Scattering in Solids V,* edited by M. Cardona and G. Guentherodt (Springer, Berlin, 1989).
[5] W. Kohn and P. Vahistha, in *Theory of the Inhomogeneous Electron Gas,* edited by S. Lundqvist and N. H. March (Plenum, New York, 1983).
[6] F. Stern, Phys. Rev. Lett. **18**, 546 (1967).
[7] S. Das Sarma and A. Madhukar, Phys. Rev. B **23**, 805 (1981); G. E. Santoro and G. F. Giuliani, Phys. Rev. B **37**, 937 (1988).
[8] D. S. Kainth *et al.,* Phys. Rev. B **59**, 2095 (1999); D. S. Kainth *et al.,* J. Phys. Condens. Matter **12**, 439 (1999).
[9] A. G. Rojo, J. Phys. Condens. Matter **11**, R31–R52 (1999).
[10] D. Neilson *et al.,* Phys. Rev. Lett. **71**, 4035 (1993).
[11] G. Kalman, V. Valtchinov, and K. I. Golden, Phys. Rev. Lett. **82**, 3124 (1999); see also the alternative approach by J. Ortner [Phys. Rev. B **59**, 9870 (1999)].
[12] D. Grecu, Phys. Rev. B **8**, 1958 (1973).
[13] S. Das Sarma and E. H. Hwang, Phys. Rev. Lett. **81**, 4216 (1998).
[14] This crossing of $\hbar\omega_{\mathrm{CDE}}$ with Δ_{SAS} for a *single quantum well* has been theoretically predicted by S. Das Sarma and I. K. Marmorkos [Phys. Rev. B **47**, 16 343 (1993)] and measured by S. Ernst, A. R. Goñi, K. Syassen, and K. Eberl [Phys. Rev. Lett. **72**, 4029 (1994)]. Our calculation indicates that such an anomalous situation persists in DQW systems.
[15] P. G. Bolcatto and C. R. Proetto, Phys. Rev. Lett. **85**, 679 (2000).
[16] Note that in the $2S$ regime, Δn and Δ_{SAS} become linked by $\Delta_{\mathrm{SAS}} = \pi\hbar^2\Delta n/m^*$.